

## Sequential NMR assignments of labile protons in DNA using two-dimensional nuclear-Overhauser-enhancement spectroscopy with three jump-and-return pulse sequences

Gottfried OTTING<sup>1</sup>, Rolf GRÜTTER<sup>1</sup>, Werner LEUPIN<sup>1</sup>, Carlo MINGANTI<sup>2</sup>, K. N. GANESH<sup>2</sup>, Brian S. SPROAT<sup>2</sup>, Michael J. GAIT<sup>2</sup> and Kurt WÜTHRICH<sup>1</sup>

<sup>1</sup> Institut für Molekularbiologie und Biophysik, Eidgenössische Technische Hochschule-Hönggerberg, Zürich

<sup>2</sup> Medical Research Council Laboratory of Molecular Biology, Cambridge

(Received November 20, 1986) – EJB 86 1233

Two-dimensional nuclear Overhauser enhancement (NOESY) spectra of labile protons were recorded in H<sub>2</sub>O solutions of a protein and of a DNA duplex, using a modification of the standard NOESY experiment with all three 90° pulses replaced by jump-and-return sequences. For the protein as well as the DNA fragment the strategically important spectral regions could be recorded with good sensitivity and free of artifacts. Using this procedure, sequence-specific assignments were obtained for the imino protons, C2H of adenine, and C4NH<sub>2</sub> of cytosine in a 23-base-pair DNA duplex which includes the 17-base-pair O<sub>R</sub>3 repressor binding site of bacteriophage λ. Based on comparison with previously published results on the isolated O<sub>R</sub>3 binding site, these data were used for a study of chain termination effects on the chemical shifts of imino proton resonances of DNA duplexes.

For <sup>1</sup>H-NMR studies of nucleic acids in H<sub>2</sub>O solution, where selective saturation (e.g. [1]) cannot be employed, a variety of different solvent suppression schemes by selective excitation have been applied with one-dimensional (1D) Fourier transform experiments [2–16]. Some of these techniques were recently also adapted for use with two-dimensional (2D) NMR, in particular 2D nuclear Overhauser enhancement spectroscopy (NOESY). Thereby, in all but one [17] of the modifications of the basic NOESY pulse sequence,

$$90^\circ - t_1 - 90^\circ - \tau_m - 90^\circ - \text{Acq.}(t_2) \quad (1)$$

only the last pulse was replaced by a semiselective excitation scheme [18–23]. This leads to a 2D excitation profile which exhibits the spectral amplitude response of the semiselective pulse along  $\omega_2$ , but is uniform along the  $\omega_1$  frequency axis. This could be very powerful with a phase program which assures that the combined effects of the first two pulses in the NOESY experiment always lead either to an effective 0-degree or 180-degree rotation at the frequency of the water resonance. The water magnetization would thus be parallel to the z-axis at all times except during  $t_1$ , but irrespective of the radio-frequency carrier position relative to the water line such phase cycles would invariably also lead to folding of the spectrum along  $\omega_1$  about the water resonance [24]. On the other hand, all experimental schemes which prevent folding of the spectrum along  $\omega_1$  include scans which bring water magnetization into the x,y plane during the mixing time  $\tau_m$ , so that after the semiselective observation pulse a huge water signal must be acquired. This situation would be less severe in experiments with a long mixing time, during which most of

the transverse magnetization could relax. Quite generally, it could also be improved with a homospoil pulse applied during the mixing time.

Different approaches can be based on the use of three semiselective pulses in the NOESY experiment [17]. The water resonance then remains essentially unexcited throughout, so that this scheme offers a maximum degree of water signal suppression for 2D experiments. A disadvantage, however, is that the excitation of the <sup>1</sup>H-NMR spectrum is no longer uniform in the  $\omega_1$  dimension. Both the excitation amplitudes and the phase characteristics along  $\omega_1$  are determined by the spectral amplitude response and by phase shifts caused by the two semiselective pulses which frame the evolution period. In phase-sensitive recordings this may necessitate large linear phase corrections, which inevitably convert the wings of large signals into a baseline roll [14]. In this note we propose a novel scheme which is free of phase shifts from the use of semiselective pulses, i.e. replacement of all three pulses in NOESY by jump-and-return pulse sequences [9]. This new NOESY scheme is then used for obtaining sequential NMR assignments for the labile protons in a DNA duplex comprising 23 base pairs.

### MATERIALS AND METHODS

The 23-base-pair DNA duplex of Fig. 1 was synthesized as two single-stranded polynucleotides by a solid-phase phosphotriester method as described previously [25]. The sodium salt of the duplex was dissolved in a 0.05 M phosphate buffer containing 0.1 M NaCl and 10% <sup>2</sup>H<sub>2</sub>O, pH 7.0. The DNA concentration was 3.6 mM in duplex. Basic pancreatic trypsin inhibitor was used as obtained from Bayer AG (Trasylo<sup>®</sup>). A 20 mM solution in 90% H<sub>2</sub>O + 10% <sup>2</sup>H<sub>2</sub>O, pH 4.3 was prepared for the NMR experiments.

Correspondence to K. Wüthrich, Institut für Molekularbiologie und Biophysik, ETH-Hönggerberg, CH-8093 Zürich, Switzerland

Abbreviations. NOESY, two-dimensional nuclear-Overhauser-enhancement spectroscopy; 1D, one-dimensional; 2D, two-dimensional.

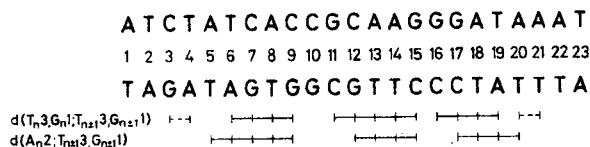


Fig. 1. Chemical structure of the 23-bp DNA containing the  $\lambda$   $O_R3$  repressor binding site (base pairs 4–20) which was used for this study. The base pair numbers referred to in the text and in Table 1 are indicated. Below the sequence the sequential NOEs used for obtaining NMR assignments of labile protons and adenine 2H are indicated. Solid lines identify NOEs seen at 310 K, broken lines those observed only at 293 K.

2D NMR spectra were recorded at 500 MHz on a Bruker WM 500 spectrometer, or at 360 MHz on a Bruker AM 360 spectrometer. For all spectra the regular NOESY phase cycle with quadrature detection was used [26, 27]. The 90° pulse width was determined by minimizing the initial data points of a free-induction decay obtained with a sequence of two 90° pulses applied in immediate succession. Spectral parameters and further experimental details are given in the figure captions.

For solvent suppression all three 90° pulses in the NOESY scheme (1) were replaced by the jump-and-return sequence

$$(90_x^\circ - \tau - 90_{-x}^\circ). \quad (2)$$

Fundamentally, the advantage of this approach relative to the earlier solvent suppression schemes for 2D NMR [17–23] stems from the fact that the jump-and-return sequence is the only semiselective pulse sequence known which causes no linear phase shifts. There are also practical benefits resulting in rapid experimental setup, since one neither needs to determine pulse widths for flip angles smaller than 90° nor to adjust pulse powers. The 2D excitation profile  $A(\omega_1, \omega_2)$  from this modification of the NOESY experiment is given by

$$A(\omega_1, \omega_2) = \sin^2(\omega_1 \tau) \sin(\omega_2 \tau) \quad (3)$$

where  $\omega_1$  and  $\omega_2$  denote the precession frequencies relative to the suppressed solvent signal during  $t_1$  and  $t_2$ , respectively. From Eqn (3), which neglects off-set effects as well as relaxation and precession due to scalar coupling during the waiting time  $\tau$ , one estimates that relative to an experiment without solvent suppression the loss of signal intensity for the DNA imino proton resonances will be less than 10%, if the first excitation maximum is set within the spectral region of the imino protons. The regular NOESY phase cycle with quadrature detection can be used [26, 27]. The 90° pulse width has to be determined rather carefully (see above), since the phase program cannot completely compensate for miss-set pulse lengths and therefore nonlinear phase shifts along both  $\omega_1$  and  $\omega_2$  might otherwise be encountered.

## RESULTS

The distribution of the  $^1\text{H}$  chemical shifts in proteins and nucleic acids [28] is sufficiently different so that experiments with both classes of compounds provide complementary information on the excitation profiles in experiments with semiselective irradiation. Therefore we used measurements with a protein and with a DNA duplex to test the solvent suppression scheme described in the preceding section. Subsequently the NOESY spectra obtained with the DNA were used for sequential assignments of the labile protons.

### Solvent suppression by the modified NOESY scheme with three jump-and-return sequences

A comparison of the NOESY experimental schemes with only the third 90° pulse, or all three 90° pulses, respectively, replaced by jump-and-return sequences is afforded by Fig. 2. Fig. 2A shows a spectrum of basic pancreatic trypsin inhibitor obtained with only the last NOESY pulse replaced by a jump-and-return sequence. Clearly, comparison with corresponding spectra recorded with water saturation (e.g. [29]) shows that the excitation is uniform along  $\omega_1$ . A stripe of exchange peaks between water and rapidly exchanging labile protons [28] can be seen near  $\omega_1 = 4.6$  ppm. Fig. 2B shows the spectrum obtained with all three pulses of the NOESY sequence replaced by jump-and-return pulse sequences. The excitation along  $\omega_1$  is modulated with a  $\sin^2$  function (Eqn 3) with maxima at intervals of about 3.5 ppm relative to the water resonance. The first maxima are thus at about 1.0 ppm and 8.0 ppm. Compared to Fig. 2A, the signal-to-noise ratio is improved in the regions near the excitation maxima, since the improved water suppression allowed the use of a higher receiver gain setting. Overall, these experiments with basic pancreatic trypsin inhibitor thus afford a good illustration of the excitation profiles for NOESY with one or three jump-and-return sequences, respectively.

The labile protons of DNA duplexes exhibit cross peaks in two quite narrow and well separated spectral regions, and therefore a non-uniform excitation profile can be selected which leads to minimal loss of information, since the spectral regions near the excitation minima do not contain resonance lines of interest. For the spectrum of Fig. 3 excitation maxima were set at 1460 Hz and 4380 Hz from the water line, corresponding to 7.7 ppm and 13.5 ppm relative to sodium 2,2-dimethyl-2-silapentane-5-sulphonate. The excitation was minimal at the water frequency of 4.8 ppm, and at 10.6 ppm. With this pattern, excitation for the imino protons over 12.0–15.0 ppm and for adenine 2H and amino protons over 6.2–9.2 ppm could be achieved simultaneously. The spectral region shown contains cross peaks between different imino protons, between imino protons and amino protons, and between imino protons and nonlabile adenine 2H. There are no exchange peaks between the imino protons and  $\text{H}_2\text{O}$ , i.e. the spectral region near  $\omega_1 = 4.8$  ppm is devoid of resonance intensity.

### Sequential assignments of labile protons in a 23-bp DNA

The 23-bp DNA studied (Fig. 1) represents a part of the operator binding region of bacteriophage  $\lambda$ , containing as the central core the 17-bp  $O_R3$  repressor binding site. The information used for obtaining the sequence-specific  $^1\text{H}$ -NMR assignments listed in Table 1 is contained in Figs 1, 4 and 5, which show, respectively, the nucleotide sequences in the 23-bp DNA, the NOE connectivities between different imino protons, between imino protons and amino protons, and between imino protons and nonlabile adenine 2H, and the intensity distribution for the imino proton lines in the 1D NMR spectrum. In addition, the amino-proton–amino-proton cross peaks in the region ( $\omega_1 = 6.1$ –6.9 ppm,  $\omega_2 = 7.8$ –8.6 ppm) of the NOESY spectrum of Fig. 3 (not shown) were analyzed for the assignment of the amino protons of cytosine.

Following previous work with different DNA fragments (e.g. [30–33]), the sequential resonance assignments of the exchangeable protons and the adenine C2 protons relied on

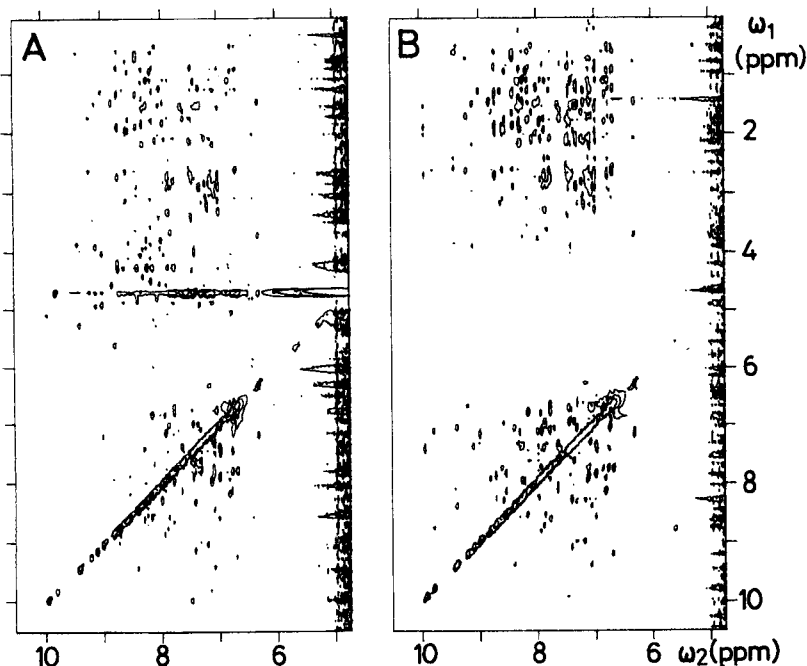


Fig. 2. 360-MHz  $^1\text{H}$ -NOESY spectra of basic pancreatic trypsin inhibitor in  $\text{H}_2\text{O}$  solution, recorded at 310 K with a mixing time of 150 ms. (A) The last pulse of the NOESY pulse sequence (1) was replaced by a jump-and-return pulse sequence (2). (B) All three  $90^\circ$  pulses were replaced by jump-and-return pulse sequences. In both experiments the carrier was set on the water resonance, and quadrature detection was used. The delay  $\tau$  in each jump-and-return pulse sequence (2) was 200  $\mu\text{s}$ , which corresponds to having a first excitation maximum about 3.5 ppm away from the water signal. In (A) a baseline correction along  $\omega_2$  using a fourth-order polynomial was applied to remove a large dispersive wing at the  $\omega_1$  frequency of the water resonance

NOE observation of short distances between hydrogen atoms within the same base pair, or in adjacent stacked base pairs. The inter-base pair distances between imino protons are of the order of 0.35 nm in B-DNA, and those between imino protons and adenine 2H are about 0.4 nm [28]. The corresponding NOEs are weak compared to the intra-base-pair NOEs, which correspond to distances of the order of 0.25 nm between imino proton and cytosine 4H, or between imino proton and adenine 2H. An important aspect of the whole assignment procedure is to identify distinct locations in the sequence of base pairs by matching the segments obtained with the sequential assignments against corresponding regions in the chemical structure (Fig. 1). Thereby it must be considered that the direction of the sequential assignments can only be determined by comparison with the chemically determined sequence.

The A · T base pair 8 is unique among all A · T base pairs in Fig. 1, since both its neighbors are G · C base pairs, and the neighbouring G · C base pairs at position 7 is again framed by two A · T base pairs. From the analysis of the imino-proton–imino-proton NOEs this unique base pair was readily identified (Fig. 4). Starting from the imino proton resonance of base pair 8, four imino proton resonances were sequentially connected, presenting a segment of four base pairs which were found to match positions 6–9 in the sequence of the 23-bp DNA (Fig. 1). These assignments were confirmed and extended to the fifth base pair by the imino-proton–adenine-2H NOEs (Fig. 4). Starting from a second, arbitrarily chosen, imino proton line of an A · T base pair, analysis of imino-proton–imino-proton and imino-proton–adenine-2H NOEs resulted in the identification of a segment of two G · C base pairs followed by three A · T base pairs,

which coincided only with the positions 16–20 in the sequence of the 23 base pairs. A third train of sequentially neighbouring imino protons was found to represent a base-pair segment  $(\text{G} \cdot \text{C})_2(\text{A} \cdot \text{T})_2\text{G} \cdot \text{C}$ , which could at this stage only be attributed to the base pairs in positions 11–15 (Fig. 1). Overall, the sequence-specific assignments at this point accounted for 15 imino protons. Integration of the 1D imino proton spectrum at 310 K showed that there was one additional resonance each of an A · T and a G · C imino proton (Fig. 5). These two lines were therefore attributed to positions 4 and 10, respectively, assuming that the three A · T base pairs at both ends of the duplex were not observed because of fraying [28, 34]. This was subsequently confirmed by the observation of two additional imino proton lines in a 1D NMR spectrum recorded in  $\text{H}_2\text{O}$  at 293 K. A NOESY experiment recorded with the same conditions showed that these additional lines gave rise to NOEs with the imino protons of base pairs 4 and 20, respectively. Furthermore, the sequence-specific assignments of adenine C2 protons in the 23-bp DNA (Fig. 1) were confirmed by observation of NOEs between adenine C2 protons in NOESY spectra recorded in  $^2\text{H}_2\text{O}$  (unpublished results).

Table 1 lists the chemical shifts of all the protons assigned by the NOESY experiment with three jump-and-return sequences. The hydrogen-bonded amino protons of cytosine were identified from the intra-base-pair NOEs with the imino protons (Fig. 4). The other amino protons of cytosine could not be unambiguously assigned from Fig. 4 because of the overlap with the amino protons of G, but their assignments resulted from the analysis of the direct amino-proton–amino-proton NOESY cross peaks (not shown).

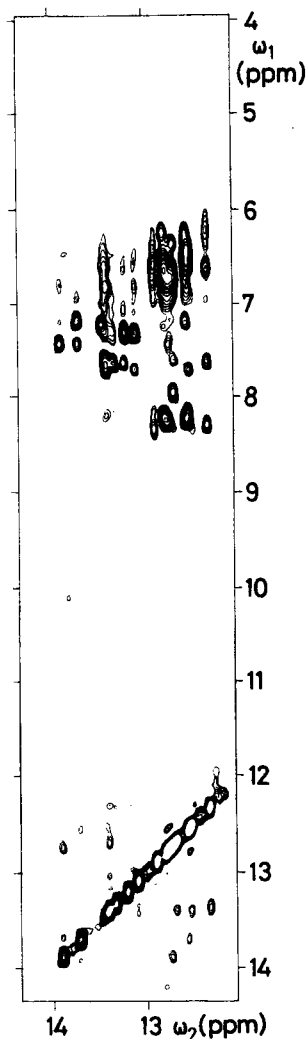


Fig. 3. Spectral region ( $\omega_2 = 12.0-14.3$  ppm,  $\omega_1 = 3.9-14.3$  ppm) of a 500-MHz  $^1\text{H}$ -NOESY spectrum of the 23-bp DNA in  $\text{H}_2\text{O}$  recorded at 310 K using three jump-and-return pulse sequences in place of the  $90^\circ$  pulses. The carrier frequency was set on the water resonance. The mixing time  $\tau_m$  was 120 ms. The delay  $\tau$  in each jump-and-return sequence was 171  $\mu\text{s}$ . 704 scans were accumulated per free induction decay, with a maximum  $t_1$  value of 13.4 ms and  $t_{2\text{max}}$  (maximum recorded length of a single transient) equal to 29.4 ms. The total experimental time was about 60 h. The time domain data were multiplied with sine bell windows shifted by  $\pi/5$  and  $\pi/3$  in  $t_2$  and  $t_1$ , respectively. In order to eliminate dispersive wings from the water line the base line was corrected before Fourier transformation along  $\omega_1$ , using a first-order polynomial

## DISCUSSION

This paper introduces the use of a modified NOESY experiment, where all three  $90^\circ$  pulses are replaced by jump-and-return sequences, for solvent suppression in experiments with  $\text{H}_2\text{O}$  solutions of proteins and nucleic acids. Compared to previously proposed solvent suppression techniques with semiselective excitation, this procedure is superior since the jump-and-return sequence does not cause linear phase shifts. While for most experiments with proteins, solvent saturation [1, 28] is probably the preferred technique, pulse schemes without water irradiation may be useful for the investigation of rapidly exchanging amide protons, for example at high pH, at high temperature, or in partially unfolded proteins. The presently proposed experiment will, however, be expected to

Table 1. Chemical shifts of imino protons, amino protons and adenine 2H in the 23-bp DNA of Fig. 1

Shifts were measured in  $\text{H}_2\text{O}$  solution,  $T = 310$  K, 0.1 M NaCl, 0.05 M phosphate buffer, pH 7.0. They are indirectly referenced to sodium 2,2-dimethyl-2-silapentane-5-sulphonate using the  $\text{H}_2\text{O}$  resonance previously calibrated in stock buffer solution

Base pair	Gua 1H	Thy 3H	Ade 2H	Cyt 4H	
				H-bonded	non- H-bonded
	ppm				
1. A · T					
2. T · A					
3. C · G	12.51 <sup>a</sup>				
4. T · A		13.47	7.21		
5. A · T		13.21	7.30		
6. T · A		13.33	7.62		
7. C · G	12.33			8.30	6.61
8. A · T		13.41	7.60		
9. C · G	12.68			7.96	6.35
10. C · G	12.89			8.36	6.57
11. G · C	12.79			8.21	6.23
12. C · G	12.56			8.27	6.23
13. A · T		13.71	7.17		
14. A · T		13.91	7.43		
15. G · C	12.72			8.27	6.77, 6.83 <sup>b</sup>
16. G · C	12.76			8.27	
17. G · C	12.52			8.18	6.58
18. A · T		13.44	7.72		
19. T · A		13.10	7.32		
20. A · T		13.40	6.82		
21. A · T		13.93 <sup>a</sup>			
22. A · T					
23. T · A					

<sup>a</sup> Observed only at 293 K, where this chemical shift was measured.

<sup>b</sup> The non-H-bonded 4H lines of C15 and C16 were not individually assigned.

be most useful for nucleic acids. This is illustrated with the relatively large (15 kDa) 23-bp DNA of Fig. 1, for which sequence-specific assignments were obtained for the imino protons, adenine 2H, and the amino protons of cytosine (Table 1).

The NMR spectrum of the isolated 17-base-pair  $\text{O}_R3$  binding site contained in the 23-bp DNA of Fig. 1 was previously studied and the resonances sequentially assigned, both in  $\text{H}_2\text{O}$  [35, 36] and  $\text{D}_2\text{O}$  [37, 38] solutions. For the labile protons these earlier assignments at ambient temperatures are necessarily incomplete because of fraying at the chain ends [34]. However, for the central 13 base pairs the results can be compared with those listed in Table 1. This comparison supports the suggestion that the sequence-specific assignments in this and the earlier studies are in full agreement. With the present experiments the sequence-specific assignments for all imino

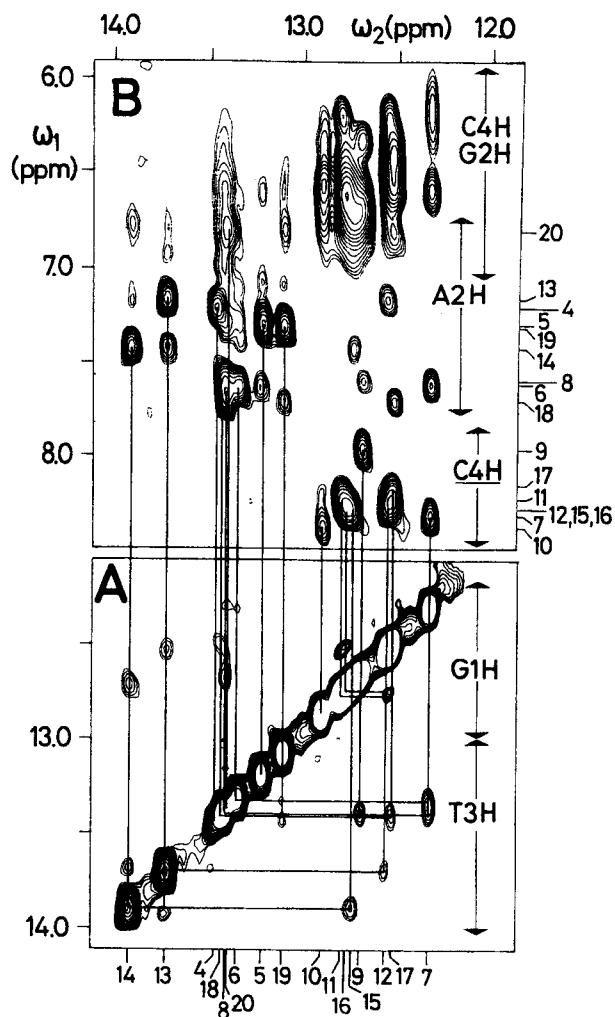


Fig. 4. Expanded plots of two regions from the spectrum in Fig. 3, with identification of NOEs between different imino protons (A), and between imino protons and adenine 2H or amino protons (B). The arrows on the right-hand side of the figure outline the chemical shift ranges for the proton types considered here. Individual imino proton chemical shifts are indicated at the bottom of the figure by the numbers of the base pairs to which they belong (Fig. 1). Similarly, individual assignments for adenine 2H and for the hydrogen-bonded amino protons of cytosine are given on the right

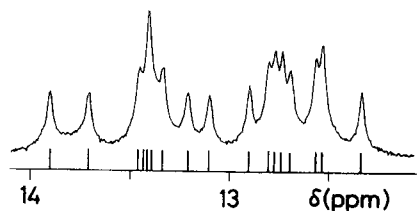


Fig. 5. Imino proton region 12.0–14.1 ppm of a 1D  $^1\text{H}$ -NMR spectrum at 310 K of the same solution of the 23-bp DNA as in Fig. 3. The stick diagram below the spectrum indicates the positions of 17 one-proton lines

and most amino protons of the entire  $\text{O}_R3$  binding site are now available.

Comparison of the NMR data for the 23-bp DNA with those of the 17-bp  $\text{O}_R3$  enables an investigation of chain termination effects on the proton resonances of a DNA

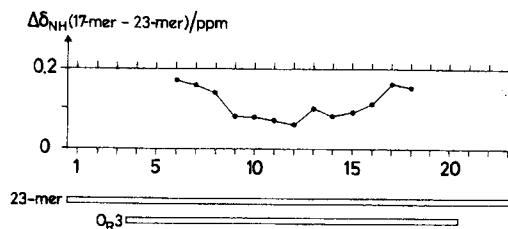


Fig. 6. Plot of the differences between corresponding imino proton chemical shifts in the 23-bp DNA and the 17-bp DNA versus the sequence of base pairs (Fig. 1). The data for this analysis are from the following sources: 23-bp DNA, present measurements at 293 K of the same solution as in Fig. 3; 17-bp DNA, measurements at 293 K [34] in a solution with 0.2 M KCl, 1 mM EDTA, 10%  $\text{D}_2\text{O}$ , 10 mM Tris buffer, pH = 7.4, at a DNA concentration of 0.7 mM in duplex. At the bottom, the figure contains a schematic drawing showing the location of the 17-bp  $\text{O}_R3$ -binding site (17-mer) relative to the 23-bp DNA (23-mer)

duplex. It is of interest that this study can be done with relatively long chains amounting to approximately two double-helical turns, since earlier investigations mainly relied on short duplexes (e.g. [39]). Fig. 6 shows a plot of the imino proton chemical shift differences versus the polynucleotide sequence. For the eight central base pairs the spread of the differences between the 23-bp and 17-bp DNAs is within 0.05 ppm. Considering that the experiments were done at different times and with somewhat different solvent conditions, this variation lies within the accuracy of the measurements. For the imino proton lines corresponding to the peripheral base pairs in the 17-bp DNA significantly larger differences were observed (whereby the imino proton resonances of the two terminal base pairs of this DNA could not be detected at 293 K due to fraying). We thus have an indication that at this temperature chain-termination effects on the chemical shifts of the labile proton resonances of a DNA double helix affect the protons of the four or five peripheral base pairs, which agrees rather well with earlier observations using different techniques [39]. This indicates that considerable care should be exercised when using results from solution studies with DNA duplexes shorter than about 10 base pairs for extrapolations to the behaviour of long DNA strands, e.g. with regard to studies of sequence effects on local conformation.

Financial support by the *Schweizerischer Nationalfonds* (project 3.198.85) is gratefully acknowledged. We thank Mrs E. Hunziker-Kwik and Mr R. Marani for the careful preparation of the figures and the manuscript.

## REFERENCES

1. Wider, G., Macura, S., Anil-Kumar, Ernst, R. R. & Wüthrich, K. (1984) *J. Magn. Reson.* **56**, 207–234.
2. Redfield, A. G. & Gupta, R. K. (1971) *J. Chem. Phys.* **54**, 1418–1419.
3. Krugh, T. R. & Schaefer, W. C. (1975) *J. Magn. Reson.* **19**, 99–107.
4. Redfield, A. G., Kunz, S. D. & Ralph, E. K. (1975) *J. Magn. Reson.* **19**, 114–117.
5. Gupta, R. K. & Gupta, P. (1979) *J. Magn. Reson.* **34**, 657–661.
6. Marshall, A. G., Marcus, T. & Sallos, J. (1979) *J. Magn. Reson.* **35**, 227–230.
7. Wright, J. M., Feigon, J., Denny, W. A., Leupin, W. & Kearns, D. R. (1981) *J. Magn. Reson.* **45**, 514–519.
8. Hore, P. J. (1983) *J. Magn. Reson.* **54**, 539–542.

9. Plateau, P. & Guéron, M. (1982) *J. Am. Chem. Soc.* **104**, 7310–7311.
10. Sklenar, V. & Starcuk, Z. (1982) *J. Magn. Reson.* **50**, 495–501.
11. Starcuk, Z. & Sklenar, V. (1985) *J. Magn. Reson.* **61**, 567–570.
12. Clore, G. M., Kimber, B. J. & Gronenborn, A. M. (1983) *J. Magn. Reson.* **54**, 170–173.
13. Morris, G. A. & Freeman, R. (1978) *J. Magn. Reson.* **29**, 433–462.
14. Plateau, P., Dumas, C. & Guéron, M. (1983) *J. Magn. Reson.* **54**, 46–53.
15. Bleich, H. & Wilde, J. (1984) *J. Magn. Reson.* **56**, 154–155.
16. Hore, P. J. (1983) *J. Magn. Reson.* **55**, 283–300.
17. Hare, D. R., Ribeiro, N. S., Wemmer, D. E. & Reid, B. R. (1985) *Biochemistry* **24**, 4300–4306.
18. Haasnoot, C. A. G., Heerschap, A. & Hilbers, C. W. (1983) *J. Am. Chem. Soc.* **105**, 5483–5484.
19. Haasnoot, C. A. G. & Hilbers, C. W. (1983) *Biopolymers* **22**, 1259–1266.
20. Heerschap, A., Mellema, J., Janssen, H. G. J. M., Walters, J. A. L. I., Haasnoot, C. A. G. & Hilbers, C. W. (1985) *Eur. J. Biochem.* **149**, 649–655.
21. Kearns, D. R., Mirau, P. A., Assa-Munt, N. & Behling, R. W. (1983) *Nucleic acids: The vectors of life*, pp. 113–125. D. Reidel Publishing Company, Dordrecht.
22. Boelens, R., Scheek, R. M., Dijkstra, K. & Kaptein, R. (1985) *J. Magn. Reson.* **62**, 378–386.
23. Dobson, C. M., Lian, L. Y., Redfield, C. & Topping, K. D. (1986) *J. Magn. Reson.* **69**, 201–209.
24. Guittet, E., Delsuc, M. A. & Lallemand, J. Y. (1984) *J. Am. Chem. Soc.* **106**, 4278–4279.
25. Minganti, C., Ganesh, K. N., Sproat, B. S. & Gait, M. J. (1985) *Anal. Biochem.* **146**, 63–74.
26. States, D. J., Haberkorn, R. A. & Ruben, D. J. (1982) *J. Magn. Reson.* **48**, 286–292.
27. Marion, D. & Wüthrich, K. (1983) *Biochem. Biophys. Res. Commun.* **113**, 967–974.
28. Wüthrich, K. (1986) *NMR of proteins and nucleic acids*, Wiley, New York.
29. Wagner, G., Braun, W., Havel, T. F., Schaumann, T., Gö, N. & Wüthrich, K. (1987) *J. Mol. Biol.*, in the press.
30. Chou, S.-H., Hare, D. R., Wemmer, D. E. & Reid, B. R. (1983) *Biochemistry* **22**, 3037–3041.
31. Lee, S. J., Akutsu, H., Kyogoku, Y., Kitano, K., Tozuka, Z., Ohta, A., Ohtsu, E. & Ikehara, M. (1983) *Nucleic Acids Res.* **12**, 197–200.
32. McConnell, B. (1984) *J. Biomol. Struct. Dyn.* **1**, 1407–1421.
33. Fazakerley, G. V., Téoule, R., Guy, A., Fritzsche, H. & Guschlbauer, W. (1985) *Biochemistry* **24**, 4540–4548.
34. Patel, D. J. & Hilbers, C. W. (1975) *Biochemistry* **14**, 2651–2660.
35. Kirpichnikov, M. P., Hahn, K. D., Buck, F., Rüterjans, H., Chernov, B. K., Kurochkin, A., Skryabin, K. G. & Bayev, A. A. (1984) *Nucleic Acids Res.* **12**, 3551–3561.
36. Ulrich, E. L., John, E.-M. N., Gough, G. R., Brunden, M. J., Gilham, P. T., Westler, W. M. & Markley, J. L. (1983) *Biochemistry* **22**, 4362–4365.
37. Wemmer, D. E., Chou, S.-H. & Reid, B. R. (1984) *J. Mol. Biol.* **180**, 41–60.
38. Hahn, K. D., Buck, F., Rüterjans, H., Chernov, B. K., Skryabin, K. G. & Kirpichnikov, M. P. (1985) *Eur. Biophys. J.* **12**, 87–95.
39. Connolly, B. A. & Eckstein, F. (1984) *Biochemistry* **23**, 5523–5527.